MULTIGRID METHOD FOR PERIODIC HETEROGENEOUS MEDIA. PART 1: CONVERGENCE STUDIES FOR ONE-DIMENSIONAL CASE

Jacob Fish and Vladimir Belsky
Department of Civil Engineering

Rensselaer Polytechnic Institute, Troy, NY 12180

ABSTRACT

A multi-grid method for a periodic heterogeneous medium in 1-D is presented. Based on the homogenization theory special intergrid transfer operators have been developed to simulate a low frequency response of the differential equations with oscillatory coefficients. The proposed multi-grid method have been proved to have a fast rate of convergence governed by the ratio $q/(4-q)$, where $0 < q \le 1$ depends on the microstructure. This estimate reveals that the rate of convergence increases as $q \to 0$, which corresponds to the increasing material heterogeneity. Numerical results have been found to be in good agreement with the theoretical estimate.

1. Introduction

The sequence of two papers presents a multi-grid method for a periodic heterogeneous medium. In the first paper we limit ourselves to 1-D problems. We believe that it is essential to demonstrate the fundamental ideas of the proposed methodology, including the mathematical formulation and convergence analysis, in one-dimensional context, first, because the rate of convergence can be only estimated in the closed form for 1-D problems and secondly, because these studies will serve as a vehicle of subsequent derivations in multidimensions. In the second paper we extend this formulation to multidimensions and incorporate adaptive features.

In the first part we consider the boundary value problem for differential equation

$$-\frac{d}{dx}\left(K\left(\frac{x}{\varepsilon}\right)\frac{d}{dx}U\right) = F(x), x \in (0, l), U(0) = 0, U(l) = 0 \qquad (1)$$

where $K(y)$ - is 1-periodic function (namely a periodic function with period 1) of $y, y = x/\varepsilon$, such that $K(y) \ge K_0 \ge 0$.

Since ε is assumed to be small, we have the differential equation with rapidly oscillatory coefficients.

The traditional approach for solving this problem uses a double scale asymptotic expansion

$$U(x, y) = U^0(x, y) + \varepsilon U^1(x, y) + \varepsilon^2 U^2(x, y) + \ldots \quad \textbf{(2)}$$

where x and $y = x/\varepsilon$ are macroscopic and microscopic co-ordinates, respectively. Under the assumption that the terms $U^k(x, y)$ are 1-periodic functions in the y variable, it is possible to obtain two separate boundary value problems. The former describes the microscopic behavior of the solution; and the latter reflects the macroscopic behavior. The fundamentals of this theory can be found, among others, in [1,2,3].

It is well known [1] that in the limit of $\varepsilon \to 0$ the solution of the source problem (1) approaches weakly in the energy norm the solution of the boundary value problem with homogenized coefficients. Unfortunately, in many practical situations when the value of ε is finite and the solution of the homogenized problem has high gradients, the homogenization theory may err badly in comparison with the exact solution of the source problem (1). The most significant errors are encountered in the portions of the problem domain where the solution has high gradients [4]. Ironically, these are precisely the regions of major interest from the practical standpoint.

One of the alternatives to homogenization is a multiscale computational approach [4]. By this technique a portion of the problem domain where homogenization procedure has been found to be inadequate by means of microscale reduction error indicators [5], is modeled entirely on the microscale, i.e., a finite element size is of the same order of magnitude as that of microconstituents. In the remaining portion of the problem domain, the details of microstructure are ignored and the finite elements are assumed to have effective material properties[3]. The system of linear equations arising from such multiscale computational technique can be solved exactly or approximately by either relaxing traction continuity or by displacement compatibility conditions between the two regions. The latter case is a typical global-local approach [6] which does not guarantee a reliable force transfer to the local region of interest. On the other hand, a solution of the coupled system of equations at several different scales may not be computationally feasible.

In this paper we propose a novel approach which takes advantage of the special nature of differential equations with oscillatory coefficients in order to develop fast iterative solvers for system of linear equations arising from such differential operators. This is accomplished using a multigrid solver with special intergrid transfer operator.

The classical multigrid approach with standard linear interpolation operators is not

well suited to approximate the lower frequency response, mainly because the lower frequency eigenvectors are not smooth in the case of differential equations with oscillatory coefficients. On the other hand, the solution based on the homogenization theory is in good agreement with the lower frequency response of the exact solution of the source problem (1). The basic idea of the proposed methodology is to construct such intergrid transfer operator so that the problem on the auxiliary grid would be identical to that with constant effective material coefficients.

The main result of the paper is states that the rate of convergence of the proposed two-grid method is mainly governed by a factor $q/(4-q)$ where $q = (\sqrt{d_1 d_2})/\frac{1}{2}(d_1 + d_2)$ and d_i represent the stiffnesses of the microconstituents. Note that if the media is homogeneous and the mesh is uniform, then $d_1 = d_2$ and one recovers the classical multigrid estimate, which states that asymtotically the error reduces by a factor of three with each new multigrid cycle. On the other hand if one phase is significantly stiffer than the other, i.e. $d_1 \gg d_2$, then the multigrid method converges in a single cycle or very few cycles at most.

The contents of the paper are as follows. Section 2 presents the multi-grid technique based on the homogenization theory. Section 3 describes the solution of the eigenvalue problem for periodic heterogeneous medium in 1-D case. These eigenvalues and eigenvectors are found in close form in order to estimate the rate of convergence of the two-grid process. In section 4 the convergence estimates are presented. In section 5 we conduct several numerical examples to study and validate the present formulation.

2. The fundamentals of multigrid method for a periodic heterogeneous medium

Consider a system of linear equations resulting from the piecewise linear finite element discretization of the source boundary value problem (1)

$$Au = f \qquad u \in R^n \qquad f \in R^n \tag{3}$$

Here A is the $n \times n$ symmetric and positive definite tridiagonal matrix; u and f are n-vector functions corresponding to the initial fine grid where each phase is discretized by at least one finite element. The boundary conditions have been incorporated into this system of equations.

Following the traditional multi-grid approach we introduce the auxiliary coarse grid. We denote the corresponding auxiliary grid functions with subscript 0. For example, u_0 denotes the nodal values of the solution in the auxiliary grid, where $u_0 \in R^m, m < n$. We also denote the prolongation operator from the coarse grid to the fine grid by Q:

$$Q: R^m \to R^n \tag{4}$$

The restriction operator Q^* from the fine-to-coarse grid is conjugated with the prolongation operator, i.e.:

$$Q^*: R^n \to R^m \tag{5}$$

We use superscripts to indicate the iteration count. Let r^i be the residual vector in the i-th iteration defined by

$$r^i = f - Au^i \tag{6}$$

where u^i - is the current approximation of the solution in the i-th iteration.

The problem of the coarse grid correction consists in the minimization of the energy functional on the subspace R^m, i.e.:

$$\begin{gathered} 1/2(A(u^i + Qu_0^i), u^i + Qu_0^i) - (f, u^i + Qu_0^i) \Rightarrow min \\ u_0^i \in R^m \end{gathered} \tag{7}$$

where (.,.) denotes the bilinear form defined by

$$(u, v) = \sum_{i=1}^{n} u_j v_j \qquad u, v \in R^n$$

A direct solution of the equation (7) yields a classical two-grid procedure. Alternatively, one may introduce an additional auxiliary grid for u_0 and so forth, leading to a natural multi-grid sequence. To fix ideas we will consider a two-grid process resulting from the direct minimization of (7)

$$A_0 u_0^i = Q^*(f - Au^i) \tag{8}$$

where $A_0 = Q^*AQ$ -is the restriction of the matrix A. The resulting classical two-grid algorithm can be written in the following manner:

a) coarse grid correction:

$$\begin{aligned} r^i &= f - Au^i \\ u_0^i &= A_0^{-1} Q^* r^i \\ \tilde{u}^i &= u^i + Qu_0^i \end{aligned} \tag{9}$$

where $\tilde{u}^i$ is a partial solution obtained after the coarse grid correction;
b) smoothing:

$$u^{i+1} = \tilde{u}^i + D(f - A\tilde{u}^i) \tag{10}$$

If the Jacobi method is employed for smoothing then

$$D = \omega(diag(A))^{-1} \tag{11}$$

where ω is a weighting factor. Note that in practice it is possible to carry out several smoothing iterations within a single coarse grid correction.
For each iteration we can associate the error vectors e^i, $\tilde{e}^i$ defined by

$$e^i = u - u^i \qquad \tilde{e}^i = u - \tilde{u}^i \tag{12}$$

where u is the exact solution of the source problem. Then the error resulting from the coarse grid correction (9) can be cast into the following form

$$\tilde{e}^i = (I - QA_0^{-1}Q^*A)e^i \tag{13}$$

where I is the identity $n \times n$ matrix. Combining equations (10),(12), the influence of smoothing on error reduction is given by:

$$e^{i+1} = (I - DA)\tilde{e}^i \tag{14}$$

and from the equations (13), (14) the error vector of the two-grid process with one post-smoothing iteration can be expressed as:

$$e^{i+1} = (I - DA)(I - QA_0^{-1}Q^*A)e^i \tag{15}$$

For subsequent derivations we will use the following notations:

$$\begin{aligned} G &= I - DA \\ T &= I - QA_0^{-1}Q^*A \end{aligned} \tag{16}$$

Then (15) can be rewritten in the following form

$$e^{i+1} = GTe^i \tag{17}$$

It is essential to note that T and $S = I - T$ are the A-ortogonal projectors [7], namely:

$$(ATw, Sv) = 0 \qquad \forall w, v \in R^n \tag{18}$$

$$\|v\|_A^2 = \|Tv\|_A^2 + \|Sv\|_A^2 \tag{19}$$

which yields that

$$\|T\|_A \leq 1 \tag{20}$$

Note that the projector T eliminates the effect of the prolongation operator, i.e.:

$$TQ = 0 \tag{21}$$

Now we will turn to the central question of how to construct a prolongation operator Q, for the case of periodic heterogeneous media, so that the auxiliary grid will not contain the details of the microstructure, but on the other hand, will accurately match the low frequency response of the source problem. Prior to answering this question, it is necessary to review some fundamental concepts of the mathematical homogenization theory.

Following the classical homogenization theory, an approximate solution of (1) can be obtained using a two-term asymptotic expansion given by

$$U(x,y) = U^{(0)}(x) + \varepsilon U^{(1)}(x,y) \tag{22}$$

where $U^{(0)}(x)$ is the solution of the homogenized boundary value problem with constant coefficients, $y = x/\varepsilon$, and

$$U^{(1)}(x,y) = H^{(1)}(y)\frac{d}{dx}U^{(0)}(x) \tag{23}$$

Here $H^{(1)}(y)$ is 1-periodic function in the y variable. Employing the classical perturbation technique [1,2,3], we obtain two uncoupled boundary value problems. The former is the problem in the function $H^{(1)}(y)$, which describes the microscopic behavior of the solution:

$$\begin{gathered} -\frac{d}{dy}\left(K(y)\frac{d}{dy}H^{(1)}(y)\right) = \frac{d}{dy}K(y) \\ 0 \leq y \leq 1 \\ H^{(1)}(0) = 0 \qquad H^{(1)}(1) = 0 \end{gathered} \tag{24}$$

The latter is the boundary value problem for the macroscopic solution

$$-\tilde{K}\frac{d^2}{dx^2}U^{(0)}(x) = F(x),\ U^{(0)}(0) = 0,\ U^{(0)}(l) = 0 \tag{25}$$

where $\tilde{K}$ - is the homogenized effective coefficient given by

$$\tilde{K} = \int_0^1 K(y)\left(\frac{d}{dy}H^{(1)} + 1\right)dy$$

For subsequent derivations we will employ the following well known relations [1-3]:

$$\begin{aligned}\tilde{K} &= \int_0^{\hat{}} K(y)\left(\frac{d}{dy}H^{(1)} + 1\right)dy = \int_0^{\hat{}} K(y)\left(\frac{d}{dy}H^{(1)} + 1\right)^2 dy \\ &= \left(\int_0^1 (K(y))^{-1}dy\right)^{-1}\end{aligned} \tag{26}$$

$$H^{(1)}(y) = \int_0^y \left(\frac{\tilde{K}}{K(\xi)} - 1\right)d\xi \tag{27}$$

The basic idea of the proposed multigrid formulation is to construct the prolongation and restriction operators on the basis of the equations (22) and (23). It will be shown that the resulting auxiliary problem would be very effective at eliminating low-frequency components of error and/or residual which are not smooth in the case of heterogeneous medium. Moreover, it will be shown that the matrix A_0 of the auxiliary system (8) corresponds to the finite element approximation of the homogenized boundary value problem with the effective coefficient (25).

Consider a one-dimensional model problem, shown in Fig. 1, which is formed by a spatial repetition of very small microstructures, or unit cells. Within the unit cell coefficient $K(y)$ is a piecewise function. The source problem is discretized with $p(p > 1)$ finite elements inside each unit cell. Each interval with $K = const$ is discretized with at least one finite element. Note that the fine grid nodes contain all the jump points of

the coefficient K. The auxiliary grid nodes coincide with the unit cell boundaries, i.e. the coarse grid nodes do not contain the jump points of the coefficient K. We denote the length of the unit cell by h_0 and the total number of unit cells by $m-1$. Then the prolongation operator Q can be expressed in the following manner:

$$[\tilde{Q}u_0]_k = [u_0]_i(1-y_j) + [u_0]_{i+1}y_j + H_j^{(1)}([u_0]_{i+1} - [u_0]_i)$$
$$k = (i-1)p + j \qquad 1 \le i \le m-1 \qquad 1 \le j \le p \tag{28}$$

where $y_j = (x_{(i-1)p+j} - x_{(i-1)p+1})/h_0$ for any i; $0 \le y_j \le 1$ are the local co-ordinates of the grid nodes inside the unit cell; $H_j^{(1)} = H^{(1)}(y_j)$ are calculated from (26), (27).

It is convenient to define the linear interpolation operator by Q, which serves as the traditional prolongation operator in the classical multi-grid approach for the second order equations. Then the proposed prolongation operator is given by

$$[\tilde{Q}u_0]_k = [Qu_0]_k + H_j^{(1)}([u_0]_{i+1} - [u_0]_i) \tag{29}$$

The coarse grid operator, A_0, can be constructed on the basis of (28). We assume that the same piecewise linear finite element shape functions are used for discretization of the initial boundary value problem (1) as well as for the unit cell problem (24). Denoting the shape functions on the fine grid by $N^j(x)$, $1 \le j \le n$, $n = (m-1)p + 1$ and using (28) we obtain the following approximation of the solution after the prolongation

$$U(x) = \sum_{i=1}^{n} N^j(x)[\tilde{Q}u_0]_j \tag{30}$$

Note that the shape functions of the auxiliary grid, $N_0^i(x)$, can be expressed as a linear combination of $N^j(x)$

$$N_0^i(x) = \sum_{i=1}^{n} N^j(x)[Qe_0^i]_j \qquad 1 \le i \le m \tag{31}$$

where $e_0^i \in R^m$ is a unit vector in the auxiliary grid, satisfying the fundamental relation of $[e_0^i]_j = \delta_{ij}$, and δ_{ij} - is the Kronecker delta. Note that $N_0^i(x)$ are the piecewise linear finite element shape functions for the auxiliary grid with a single finite element in each unit cell. Derivative approximation on each element i in the auxiliary grid is given by

$$[u'_0] = \left[\sum_{i=1}^{m} (N_0^i)'[u_0]_i \right]_k = \frac{([u_0]_{k+1} - [u_0]_k)}{h_0} \qquad (32)$$

$$1 \le k \le m-1$$

Combining (29) - (32) we obtain the following expression for the approximate solution after prolongation

$$U(x) = \sum_{i=1}^{m} (N_0^i)[u_0]_i + \sum_{i=1}^{m-1} \sum_{i=1}^{p+1} N^{(i-1)p+j}(x) H_j^{(1)} h_0 \left[\sum_{k=1}^{m} (N_0^k)'[u_0]_k \right]_i \qquad (33)$$

Note that periodicity implies that

$$N^{(i-1)p+j}(x) = N^j(h_0 y) = \tilde{N}^j(y)$$

$$1 \le j \le p \qquad y = \frac{x}{h_0} - (i-1) \qquad 0 \le y \le 1 \qquad \forall i,\ 1 \le i \le m-1 \qquad (34)$$

Differentiation of (33) and accounting for periodicity (34), yields

$$U'(x) = \sum_{i=1}^{p+1} (N_0^i)'[u_0]_i \left(1 + \frac{d}{dy} H^{(1)}(y) \right) \qquad (35)$$

where $\frac{d}{dy} H^{(1)}(y) = \sum_i \frac{d}{dy} \tilde{N}^j(y) (H_j)^{(1)}$ and $H_j^{(1)}$ is the discrete solution of the microscopic problem (24) at the FE nodes y_j, which is obtained on the basis of the finite element shape functions $\tilde{N}^j(y)$.

Finally, auxiliary grid discrete operator A_0 can be obtained by combining (30), (35) and (26), which yields

$$[A_0]_{ij} = \sum_{p=1}\sum_{q=1}\left(\int_0 K\left(\frac{x}{\varepsilon}\right)N^p(x)N^q(x)dx\right)[\tilde{Q}e_0^i]_p[\tilde{Q}e_0^j]_q$$

$$= \int_0^l\left(\int_0^1 K(y)\left(\frac{d}{dy}H^{(1)}+1\right)^2 dy\right)(N_0^i(x))'(N_0^j(x))'dx \qquad \textbf{(36)}$$

$$= \int^l \tilde{K}(N_0^i(x))'(N_0^j(x))'dx \qquad 1 \le i \le m \qquad 1 \le j \le m$$

It can be seen that the restriction of the source matrix A using the prolongation operator (28) corresponds to the finite element approximation of the boundary value problem (25) with the effective coefficient.

3. The eigenvalue problem for the periodic heterogeneous medium in 1-D case

This section deals with the eigenvalue analysis of the model boundary value problem with the periodic coefficient

$$-\frac{d}{dx}\left(K\left(\frac{x}{\varepsilon}\right)\frac{d}{dx}U\right) = \lambda U, x \in (0, l), U(0) = 0, U(l) = 0 \qquad \textbf{(37)}$$

where $K(y)$ is chosen as follows:

$$K(y) = \begin{cases} K_1, 0 \le y \le (1-\alpha) \\ K_2, (1-\alpha) \le y \le 1 \end{cases} \qquad \textbf{(38)}$$

and α represents the volume fraction, $0 \le \alpha \le 1$.

In the following we present a closed form solution of a discretization of the eigenvalue problem (37), (38), which is required for estimating the rate of convergence of the proposed two-grid method.

The eigenvalue problem defined by (37), (38) is discretized with two elements on each unit cell as shown in Fig. 2. Nodal values corresponding to the boundaries of the unit cells are denoted by u_i, $1 \le i \le m$, while the corresponding nodal values inside the unit cells are defined by $u_{i,\,i+1}$, $1 \le i \le m-1$. The number of the unit cells is $m-1$.

The effective material properties, $\tilde{K}$, for a model problem defined by (38) follow

immediately from (26)

$$\tilde{K} = \frac{K_1 K_2}{K_2(1-\alpha) + K_1 \alpha} \tag{39}$$

Proposition 1

Consider a heterogeneous medium formed by a special repetition of the unit cell (38). Each unit cell is discretized with two elements as shown in Fig. 2. Let $(\hat{\varphi}^k, \hat{\lambda}^k)$, $1 \le k \le \tilde{m} - 1$, $\tilde{m} = m - 1$, be the eigenvectors and the eigenvalues of the discretized eigenvalue problem with the homogenized effective coefficient (39), and let $\varphi^k_{i,\,i+1}$, $1 \le i \le m - 1$ be a result of prolongation of the vector $\hat{\varphi}^k$ to the interior node in the unit cell i in accordance with (28) and (27), i.e.:

$$\varphi^k_{i,\,i+1} = \beta \varphi^k_i + (1-\beta)\varphi^k_{i+1} \tag{40}$$

where

$$\beta = \frac{d_1}{d_1 + d_2},\ d_1 = K_1 \alpha,\ d_2 = K_2(1-\alpha) \tag{41}$$

Furthermore, let (φ^k, λ^k), $1 \le k \le \tilde{n} - 1$, $\tilde{n} = 2\tilde{m}$ be the eigenvectors and the eigenvalues of the discretized problem (37), (38).

Then the Proposition 1 claims that the eigenvectors and the eigenvalues of the one-dimensional problem in the heterogeneous medium (37), (38) are given by

$$\lambda^k = \frac{b^k}{b^k + 1}\hat{\lambda}^k$$

$$\varphi_i^k = \hat{\varphi}_i^k,\ 1 \le i \le m \qquad \varphi_{i,\,i+1}^k = b^k \hat{\varphi}_{i,\,i+1}^k,\ 1 \le i \le m-1$$

$$\lambda^{\tilde{n}-k} = \frac{b^k}{b^k - 1}\hat{\lambda}^k \tag{42}$$

$$\varphi_i^{\tilde{n}-k} = -\hat{\varphi}_i^k,\ 1 \le i \le m \qquad \varphi_{i,\,i+1}^{\tilde{n}-k} = b^k \hat{\varphi}_{i,\,i+1}^k,\ 1 \le i \le m-1$$

$$\lambda^{\tilde{m}} = \frac{d_1 + d_2}{\alpha(1-\alpha)h_0}$$

$$\varphi_i^{\tilde{m}} = 0,\ 1 \le i \le m \qquad \varphi_{1,\,2}^{\tilde{m}} = 1 \qquad \varphi_{i,\,i+1}^{\tilde{m}} = -\frac{d_2}{d_1}\varphi_{i-1,\,i}^{\tilde{m}},\ 2 \le i \le m-1$$

where

$$b^k = \frac{1}{\left(1 - q\hat{\lambda}^k \frac{h_0}{4\tilde{K}}\right)^{1/2}} \qquad q = 4\beta(1-\beta) \tag{43}$$

$$\hat{\lambda}^k = \frac{4\tilde{K}}{h} sin^2\left(\frac{k\pi}{2\tilde{m}}\right)$$

$$\hat{\varphi}_i^k = sin\left(\frac{(i-1)k\pi}{\tilde{m}}\right),\ 1 \le i \le m \tag{44}$$

$$1 \le k \le \tilde{m} - 1$$

Proof of Proposition 1

Consider the discretization of the eigenvalue problem (37), (38) on the basis of the linear finite elements:

$$\begin{cases} -\dfrac{K_1}{(1-\alpha)h_0}\varphi_i^k + \dfrac{K_1\alpha + K_2(1-\alpha)}{\alpha(1-\alpha)h_0}\varphi_{i,\,i+1}^k - \dfrac{K_2}{\alpha h_0}\varphi_{i+1}^k = \lambda^k\varphi_{i,\,i+1}^k \\ 1 \le i \le m-1 \\ -\dfrac{K_2}{\alpha h_0}\varphi_{i-1,\,i}^k + \dfrac{K_1\alpha + K_2(1-\alpha)}{\alpha(1-\alpha)h_0}\varphi_i^k - \dfrac{K_1}{(1-\alpha)h_0}\varphi_{i,\,i+1}^k = \lambda^k\varphi_i^k \\ 2 \le i \le m-1 \\ \varphi_1^k = 0 \qquad \varphi_m^k = 0 \\ 1 \le k \le \tilde{n}-1 \end{cases} \tag{45}$$

Inserting (41) into (45) yields

$$\begin{cases} \varphi_{i,\,i+1}^k - (\beta\varphi_i^k + (1-\beta)\varphi_{i+1}^k) = \tilde{\lambda}^k\varphi_{i,\,i+1}^k & 1 \le i \le m-1 \\ \varphi_i^k - ((1-\beta)\varphi_{i-1,\,i}^k + \beta\varphi_{i,\,i+1}^k) = \tilde{\lambda}^k\varphi_i^k & 2 \le i \le m-1 \\ \varphi_1^k = 0 \qquad \varphi_m^k = 0 & 1 \le k \le \tilde{n}-1 \end{cases} \tag{46}$$

where

$$\tilde{\lambda}^k = \frac{\alpha(1-\alpha)h_0}{d_1 + d_2}\lambda^k$$

Taking the following expression from (42)

$$\begin{aligned} \varphi_i^k &= \hat{\varphi}_i^k & 1 \le i \le m \\ \varphi_{i,\,i+1}^k &= b\hat{\varphi}_{i,\,i+1}^k & 1 \le i \le m-1 \\ & & 1 \le k \le \tilde{m}-1 \end{aligned}$$

and combining it with (40) and (46) yields

$$\begin{cases} (b-1)\hat{\varphi}^k_{i,i+1} = \tilde{\lambda}^k b\hat{\varphi}^k_{i,i+1} & 1 \le i \le m-1 \\ -\hat{\varphi}^k_{i-1} + 2\hat{\varphi}^k_i - \hat{\varphi}^k_{i+1} = \dfrac{\tilde{\lambda}^k + b - 1}{b(1-\beta)\beta}\hat{\varphi}^k_i & 2 \le i \le m-1 \\ \hat{\varphi}^k_1 = 0 \qquad \hat{\varphi}^k_m = 0 & 1 \le k \le \tilde{m}-1 \end{cases}$$

The above can be satisfied for any eigenvector, $\hat{\varphi}^k$, of the homogenized problem if, and only if, the following holds

$$\begin{cases} (b-1) = \tilde{\lambda}^k b \\ \dfrac{\hat{\lambda}^k h_0}{\tilde{K}} = \dfrac{\tilde{\lambda}^k + b - 1}{b(1-\beta)\beta} \end{cases}$$

from where follows

$$b = \pm\frac{1}{\left(1-\beta(1-\beta)\dfrac{\hat{\lambda}^k h_0}{\tilde{K}}\right)^{1/2}} \qquad \tilde{\lambda}^k = \frac{b-1}{b}$$

$$\lambda^k = \frac{b-1}{b}\frac{d_1+d_2}{\alpha(1-\alpha)h_0} = \frac{b}{b+1}\hat{\lambda}^k$$

The positive values of b lead to the eigenvalues and eigenvectors of the form given in (42) with $b^k = b$, while the negative values of b correspond to $b^k = -b$.

The middle eigenvalue and eigenvector $\tilde{m}$ in (42) follows directly from the eigenvalue problem (45). The eigenvalues and eigenvectors for the homogenized discrete eigenvalue problem can be found, among others, in [8]. □

To this end, we summarize the results of this section in the following compact notation

$$
\begin{cases}
\lambda^k = \dfrac{4\tilde{K}}{h_0} \dfrac{\sin^2\left(\dfrac{k\pi}{2\tilde{m}}\right)}{1+\left(1-q\sin^2\left(\dfrac{k\pi}{2\tilde{m}}\right)\right)^{1/2}} \\
\lambda^{2\tilde{m}-k} = \dfrac{4\tilde{K}}{h_0} \dfrac{\sin^2\left(\dfrac{k\pi}{2\tilde{m}}\right)}{1-\left(1-q\sin^2\left(\dfrac{k\pi}{2\tilde{m}}\right)\right)^{1/2}} \\
\lambda^{\tilde{m}} = \dfrac{4\tilde{K}}{h_0}\dfrac{1}{q} \\
b^k = \dfrac{1}{\left(1-q\sin^2\left(\dfrac{k\pi}{2\tilde{m}}\right)\right)^{1/2}} \\
1 \le k \le \tilde{m}-1
\end{cases}
\tag{47}
$$

where

$$
q = \frac{4d_1d_2}{(d_1+d_2)^2} \qquad 0 < q \le 1
$$

4. Evaluation of the operator T and the estimation of the rate of convergence

In this section we will estimate the rate of convergence of the simple two-grid method applied to the heterogeneous medium (38). In estimating the rate of convergence, the critical step is to find a closed form expression for $T\varphi^k$, where T is the A-orthogonal projector (16) and φ^k are the eigenvectors (42). The result of this product is given in Proposition 2.

Proposition 2

Let T be the A-orthogonal projector (16); $(\varphi^k, \varphi^{\tilde{n}-k})$, $1 \le k \le \tilde{m}-1$ and $\varphi^{\tilde{m}}$ be the corresponding eigenvectors given in (42); b^k, $1 \le k \le \tilde{m}-1$ be the coefficients defined by (43). Then

$$
\begin{aligned}
T\varphi^k &= \frac{b^k - 1}{2b^k}(\varphi^k + \varphi^{\tilde{n}-k}) \\
T\varphi^{\tilde{n}-k} &= \frac{b^k + 1}{2b^k}(\varphi^k + \varphi^{\tilde{n}-k}) \qquad \textbf{(48)} \\
1 &\le k \le \tilde{m} - 1 \\
T\varphi^{\tilde{m}} &= \varphi^{\tilde{m}}
\end{aligned}
$$

where we have used the prolongation and restriction operators defined by (28),(40),(41):

$$
\tilde{Q} = \begin{bmatrix}
1 & & & & \\
\beta & 1-\beta & & & \\
 & 1 & & & \\
 & \beta & 1-\beta & & \\
 & & 1 & & \\
\cdots & \cdots & \cdots & \cdots & \cdots \\
 & & & \beta & 1-\beta \\
 & & & & 1
\end{bmatrix} \qquad \textbf{(49)}
$$

$$
\tilde{Q}^* = \begin{bmatrix}
1 & \beta & & & & & & \\
 & 1-\beta & 1 & \beta & & & & \\
 & & & 1-\beta & 1 & \beta & & \\
\cdots & \cdots & \cdots & \cdots & \cdots & \cdots & \cdots & \cdots \\
 & & & & & & 1-\beta & 1
\end{bmatrix} \qquad \textbf{(50)}
$$

and β is given in (41).

Proof of Proposition 2

Applying the operator (16) to the eigenvectors given in (42) yields

$$
T\varphi^k = (I - \tilde{Q}A_0^{-1}\tilde{Q}^*A)\varphi^k \qquad 1 \le k \le \tilde{n} - 1 \qquad \textbf{(51)}
$$

where

$$\begin{cases} A\varphi^k = \dfrac{b^k}{b^k+1}\hat{\lambda}^k\varphi^k \\ A\varphi^{\tilde{n}-k} = \dfrac{b^k}{b^k-1}\hat{\lambda}^k\varphi^{\tilde{n}-k} \\ 1 \le k \le \tilde{m}-1 \end{cases}$$

$$A\varphi^{\tilde{m}} = \lambda^{\tilde{m}}\varphi^{\tilde{m}}$$

Furthermore, inserting (40) - (43) into (50) gives

$$\begin{cases} [\tilde{Q}^*\varphi^k]_i = \left(-b^k\beta(1-\beta)\hat{\lambda}^k\dfrac{h_0}{\tilde{K}} + b^k + 1\right)\hat{\varphi}_i^k = \dfrac{b^k+1}{b^k}\hat{\varphi}_i^k \\ [\tilde{Q}^*\varphi^{\tilde{n}-k}]_i = \left(-b^k\beta(1-\beta)\hat{\lambda}^k\dfrac{h_0}{\tilde{K}} + b^k - 1\right)\hat{\varphi}_i^k = -\dfrac{b^k-1}{b^k}\hat{\varphi}_i^k \\ 1 \le i \le \tilde{m} \qquad 1 \le k \le \tilde{m}-1 \end{cases} \tag{52}$$

$$[\tilde{Q}^*\varphi^{\tilde{m}}]_i = \left(1-\beta-\frac{d_2}{d_1}\beta\right)\hat{\varphi}_{i-1,i}^{\tilde{m}} = 0 \qquad 1 \le i \le \tilde{m}$$

Combining (51) and (52) yields

$$\begin{cases} \tilde{Q}^*A\varphi^k = \hat{\lambda}^k\hat{\varphi}^k \\ \tilde{Q}^*A\varphi^{\tilde{n}-k} = -\hat{\lambda}^k\hat{\varphi}^k \end{cases} \qquad 1 \le k \le \tilde{m}-1$$

$$\tilde{Q}^*A\varphi^{\tilde{m}} = 0$$

and

$$\begin{cases} A_0^{-1}\tilde{Q}^* A\varphi^k = \hat{\varphi}^k & \\ A_0^{-1}\tilde{Q}^* A\varphi^{\tilde{n}-k} = -\hat{\varphi}^k & 1 \le k \le \tilde{m}-1 \end{cases} \tag{53}$$

$$A_0^{-1}\tilde{Q}^* A\varphi^{\tilde{m}} = 0$$

The prolongation of the eigenvectors for the auxiliary eigenvalue problem on the basis of the prolongation operator (49) can be written as follows:

$$\begin{cases} [\tilde{Q}\hat{\varphi}^k]_{i,\,i+1} = \beta\hat{\varphi}_i^k + (1-\beta)\hat{\varphi}_{i+1}^k = \hat{\varphi}_{i,\,i+1}^k = \dfrac{1}{b^k}\varphi_{i,\,i+1}^k = \dfrac{1}{b^k}\varphi_{i,\,i+1}^{\tilde{n}-k} & \\ 1 \le i \le \tilde{m} & \\ [\tilde{Q}\hat{\varphi}^k]_i = \hat{\varphi}_i^k = \varphi_i^k = -\varphi_i^{\tilde{n}-k} \qquad 1 \le i \le m \qquad 1 \le k \le \tilde{m}-1 & \end{cases} \tag{54}$$

and finally, inserting (54) into (51) yields

$$\begin{cases} [T\varphi^k]_{i,\,i+1} = \dfrac{b^k-1}{b^k}\varphi_{i,\,i+1}^k & \\ & 1 \le i \le \tilde{m} \\ [T\varphi^{\tilde{n}-k}]_{i,\,i+1} = \dfrac{b^k+1}{b^k}\varphi_{i,\,i+1}^{\tilde{n}-k} & 1 \le k \le \tilde{m}-1 \\ [T\varphi^k]_i = [T\varphi^{\tilde{n}-k}]_i = 0 \qquad 1 \le i \le m & \end{cases} \tag{55}$$

Thus, using the equalities stating that $\varphi_{i,\,i+1}^k = \varphi_{i,\,i+1}^{\tilde{n}-k}$ and $\varphi_i^k = -\varphi_i^{\tilde{n}-k}$ in (55) results in (48), which completes the proof of the Proposition 2. □

We now turn to the estimation of the rate of convergence, which is given in the Proposition 3.

Proposition 3

Let the error vector e^i in the i-th iteration of the two-grid process with one post-smoothing Jacobi iteration be represented as the linear combination of the eigenvectors (42):

$$e^i = \sum_{k=1}^{m-1} (a^i{}_k \varphi^k + a^i{}_{\tilde{n}-k} \varphi^{\tilde{n}-k}) + a^i{}_{\tilde{m}} \varphi^{\tilde{m}} \tag{56}$$

and let's introduce the following notation:

$$S_k^i = a_k^i \frac{b^k - 1}{2b^k} + a_{n-k}^i \frac{b^k + 1}{2b^k} \qquad 1 \le k \le \tilde{m} - 1 \tag{57}$$

Then

$$\begin{cases} a_k^{i+1} = S_k^i \left(1 - \omega q \frac{b^k}{b^k + 1} sin^2\left(\frac{k\pi}{2\tilde{m}}\right)\right) \\ a_{n-k}^{i+1} = S_k^i \left(1 - \omega q \frac{b^k}{b^k - 1} sin^2\left(\frac{k\pi}{2\tilde{m}}\right)\right) \end{cases} \qquad 1 \le k \le \tilde{m} - 1 \tag{58}$$

$$a_m^{i+1} = a_m^i (1 - \omega)$$

where

$$S_k^{i+1} = S_k^i \left(1 - \omega \left(2 - q\, sin^2\left(\frac{k\pi}{2\tilde{m}}\right)\right)\right) \qquad 1 \le k \le \tilde{m} - 1 \tag{59}$$

and ω - is a weighting factor of the Jacobi method.

Proof of Proposition 3

Inserting (48) into (56) and using the notation (57), yield

$$\begin{aligned} Te^i &= \sum_{k=1}^{\tilde{m}-1} \left(a_k^i \frac{b^k - 1}{2b^k} + a_{n-k}^i \frac{b^k + 1}{2b^k}\right)(\varphi^k + \varphi^{\tilde{n}-k}) + a_{\tilde{m}}^i \varphi^{\tilde{m}} \\ &= \sum_{k=1}^{\tilde{m}-1} S_k^i (\varphi^k + \varphi^{\tilde{n}-k}) + a_{\tilde{m}}^i \varphi^{\tilde{m}} \end{aligned} \tag{60}$$

Applying a single Jacobi iteration (14) to the eigenvectors given in (42) results in the following

$$G\varphi^k = (I - DA)\varphi^k = \left(1 - \omega\frac{\alpha(1-\alpha)h_0}{d_1 + d_2}\lambda^k\right)\varphi^k \qquad 1 \le k \le \tilde{n} - 1 \tag{61}$$

Inserting the eigenvalues defined in (42) into (61) and using (39), (41), (43) yields

$$\begin{cases} G\varphi^k = \left(1 - \omega q\frac{b^k}{b^k + 1}sin^2\left(\frac{k\pi}{2\tilde{m}}\right)\right)\varphi^k \\ G\varphi^{\tilde{n}-k} = \left(1 - \omega q\frac{b^k}{b^k - 1}sin^2\left(\frac{k\pi}{2\tilde{m}}\right)\right)\varphi^{\tilde{n}-k} \end{cases} \qquad 1 \le k \le \tilde{m} - 1 \tag{62}$$

$$G\varphi^{\tilde{m}} = (1 - \omega)\varphi^{\tilde{m}}$$

Combining (60) and (62) yields (58), where the value of S_k^{i+1} is found on the basis of (57)

$$S_k^{i+1} = S_k^i\left(1 - \omega q\frac{(b^k)^2 + 1}{(b^k)^2 - 1}sin^2\left(\frac{k\pi}{2\tilde{m}}\right)\right) \qquad 1 \le k \le \tilde{m} - 1 \tag{63}$$

Finally, inserting (43) and (44) into (63) results in (59), which completes the proof of the Proposition 3. □

We are now in a position to estimate the rate of convergence on the basis of eigenvalue distribution and the main results given in (47), (56) - (59).

Note that the parameter q (see (41), (43)) can be viewed as a measure of material heterogeneity. For example, the case of $q = 1$ is equivalent to the problem in a homogeneous medium, in the sense that $K_1\alpha = K_2(1-\alpha)$. Material heterogeneity increases with decreasing the value of parameter q.

Table 1 illustrates the spectrum of eigenvalues for different values of q. It can be seen that eigenvalues are clustered in two regions (except for the middle eigenvalue, which is equal to $(4K/h_0)(1/q)$). The spectral width of the two regions (defined by the difference of the maximum and minimum eigenvalues in the corresponding region) decreases with the decreasing value of q. This clustering of eigenvalues is one of the key reasons for a faster rate of convergence of the two grid process with decreasing the value of q.

We next investigate what is the weighting factor ω^* that maximize the asymptotic rate of convergence in the absence of the error component corresponding to the middle

eigenvalue, i.e., $a_{\tilde{m}} = 0$. From (59) follows

$$1 - \omega^*(2 - q) = -(1 - 2\omega^*)$$

$$or \qquad \omega^* = \frac{2}{4 - q} \qquad 1/2 < \omega^* \le 2/3 \tag{64}$$

Inserting (64) into (59) yields the following estimate of the asymptotic rate of convergence governed by the ratio $\rho = max_k \left| S_k^{i+1} / S_k^i \right|$:

$$\rho(\omega) = max_k \left| 1 - \omega \left(2 - q \, sin^2 \left(\frac{k\pi}{2\tilde{m}} \right) \right) \right|$$

$$\rho^* = \frac{q}{4 - q} \qquad 0 < \rho^* \le 1/3 \tag{65}$$

where $\omega^* = 2/3$ and $\rho^* = 1/3$ correspond to the solution of homogeneous problem. It can be seen from (65) that the asymptotic rate of convergence of the two-grid method increases (or ρ^* decreases) with decreasing the value of q (or increasing material heterogeneity).

However, if the error component corresponding to the middle eigenvalue in (58) is taken into account it is necessary to employ $\omega^{**} = 2/3$ resulting in the asymptotic rate of convergence governed by $\rho^{**} = 1/3$. So in the worse scenario we may expect the same rate of convergence as for the homogeneous problem.

The oscillatory nature of the middle eigenvector, $\varphi^{\tilde{m}}$, is described by (42). It can be seen that the eigenvector vanishes on the unit cell boundaries, but oscillates between the unit cell midside nodes in geometric progression with a negative factor depending on material heterogeneity, d_2/d_1. Such oscillatory response is unlikely to be triggered, and thus in practice the rate of convergence is governed by the estimate given in (65).

5. Numerical examples

First, we will analyze the two-grid process for solving the boundary value problem (1),(38) on the basis of uniform finite element grid with two elements on each unit cell as described in section 3 with $\alpha = 0.5$. For the purpose of simulating the singular loading the right hand side function $F(x)$ has been chosen as follows

$$F(x) = \frac{sign(x - l/2)}{|x - l/2| + \delta} \tag{66}$$

where $\delta = 10^{-8}$ and

$$sign(a) = \begin{cases} 1 & if \quad a > 0 \\ -1 & if \quad a < 0 \\ 0 & if \quad a = 0 \end{cases}$$

We carry out the smoothing iterations on the basis of the Gauss-Seidel method. As a termination criterion we use the following tolerance to bound the ratio of the residual norm versus the norm of the right hand side vector, i.e.,

$$\frac{\|r\|_1}{\|f\|_1} \leq 10^{-8} \tag{67}$$

where $\|v\|_1 = \sum_{i=1}^{n} |v_i| \qquad v \in R^n$.

The results of the numerical experiment are presented in the Table 2, where ρ_{100} and ρ_{1000} characterize the asymptotic rates of convergence for the cases with 100 and 1000 unit cells, respectively. It can be seen that the theoretical rate of convergence (65) ignoring the error component corresponding to the middle eigenvalue agrees well with the numerical result. In both cases the error is rapidly decreasing. On the other hand, the rate of convergence of the multi-grid process with conventional intergrid transfer operators is governed by the value of ρ^{conv}, which is very close to unity $(\rho^{conv} = 0.923 \div 0.992)$, indicating very slow rate of convergence. Furthermore, the rate of convergence of the conventional multi-grid process decreases as material heterogeneity increases. This is in contrast to the proposed multi-grid process where the rate of convergence improves with increase in material heterogeneity.

We next consider the same problem with 10 finite elements on each unit cell. The results of this experiment are presented in Table 3. They show that the convergence increases with decreasing the value of the parameter q. Note that the case $K_1/K_2 = 1/1$ corresponds to the standard two-grid method for the boundary value problem with constant coefficient.

The next example deals with the nonuniform fine grid. We use 10 finite elements for

the two unit cells, where the solution has a high gradient. In the remaining region we use one element per unit cell, with a homogenized effective coefficient. The ratio of $K_1/K_2 = 1/100$ is considered (Fig. 3). The results of this experiment are shown in Table 4.

The last numerical experiment deals with the three-grid method for the previously defined problem. We use here the additional coarse grid for solving the auxiliary homogenized problem and a standard multi-grid technique for formulating the coarse grid problem. The results of this experiment are shown in Table 5, where ν_1 and ν_2 are the number of pre- and post- smoothing iterations on the fine grid; ν_1^0 and ν_2^0 the corresponding values on the auxiliary grid; N_e the number of finite elements in the finest grid; N_c the number of unit cells; N_0 the number of the elements in the coarsest grid. Results of this experiment are consistent with our previous observations, and confirm our theoretical estimates given in (65).

6. Acknowledgments

The authors wish to thank the referee for his comments on the manuscript. The comparison with the conventional multi-grid method as well as the introduction of the appropriate notation were incorporated at his suggestion.

The support of NASA Langley Research Center under grant NAG-1-1356, and the National Science Foundation NYI award ECS-9257203 are gratefully acknowledged.

References

1. A. Benssousan, J.L. Lions and G. Papanicoulau, Asymptotic analysis for periodic structures, North Holland, Amsterdam, 1978.

2. E. Sanchez-Palencia and A. Zaoui, Homogenization techniques for composites. Homogenization techniques for composite media, Springer-Verlag, Berlin, 1985.

3. N.S. Bakhvalov and G.P. Panasenko, Homogenization of periodic medium processes, Nauka, Moscow, 1984.

4. J. Fish and A. Wagiman, Multiscale finite element method for a locally nonperiodic heterogeneous medium, Computational Mechanics: The International Journal 21 (1993) 1-17.

5. J. Fish, P. Nayak and M.H. Holmes, Microscale reduction error indicators and estimators for a periodic heterogeneous medium, to appear in International Journal of Numerical Methods in Engineering.

6. S.B. Dong, Global-local finite element methods, in: A.K.Noor and W.D.Pilkey, eds., State-of-the-Art Surveys on Finite Element Technology (ASME, New York, 1983) 451-474.

7. S.F. McCormick, Multigrid methods for variational problems: further results, SIAM J. Numer. Anal. 21 (1984) 255-263.

8. W.L. Briggs, A multigrid tutorial, SIAM, Philadelphia, 1987.

Fig. 1

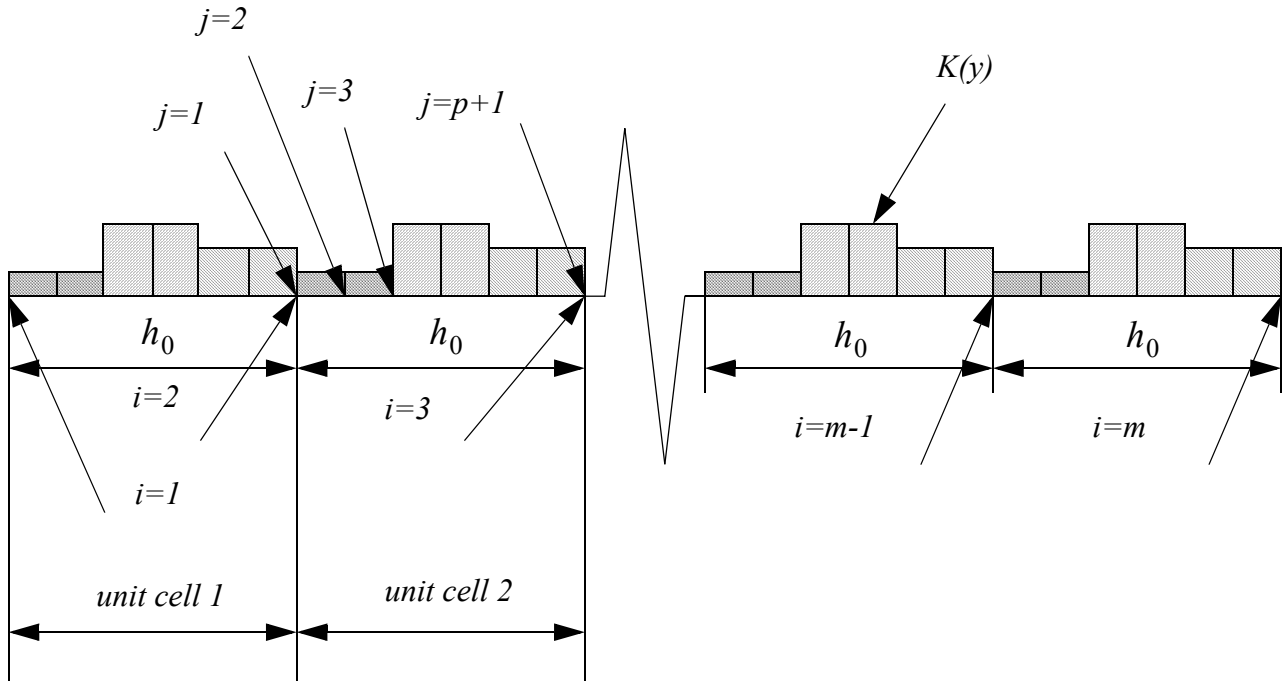

Fig. 2

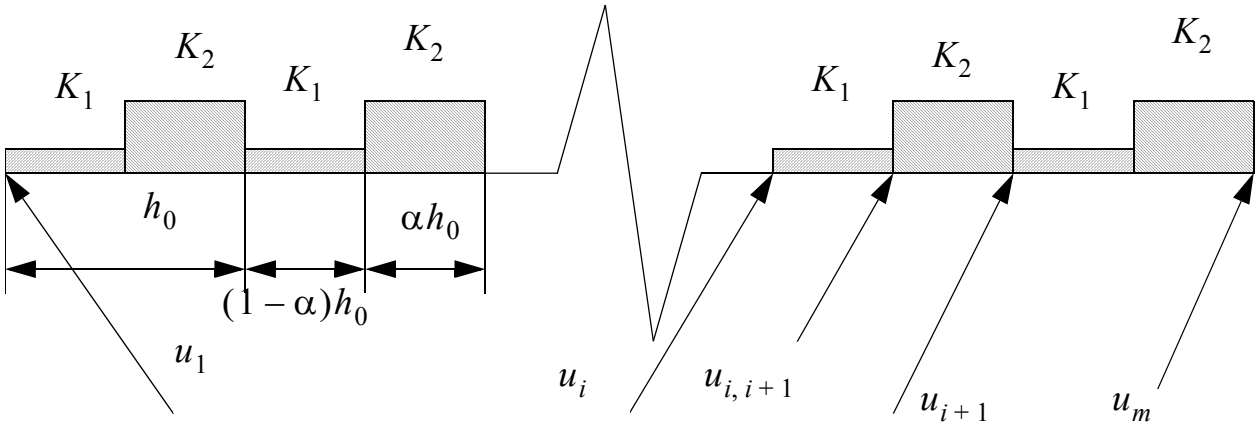

Fig. 3

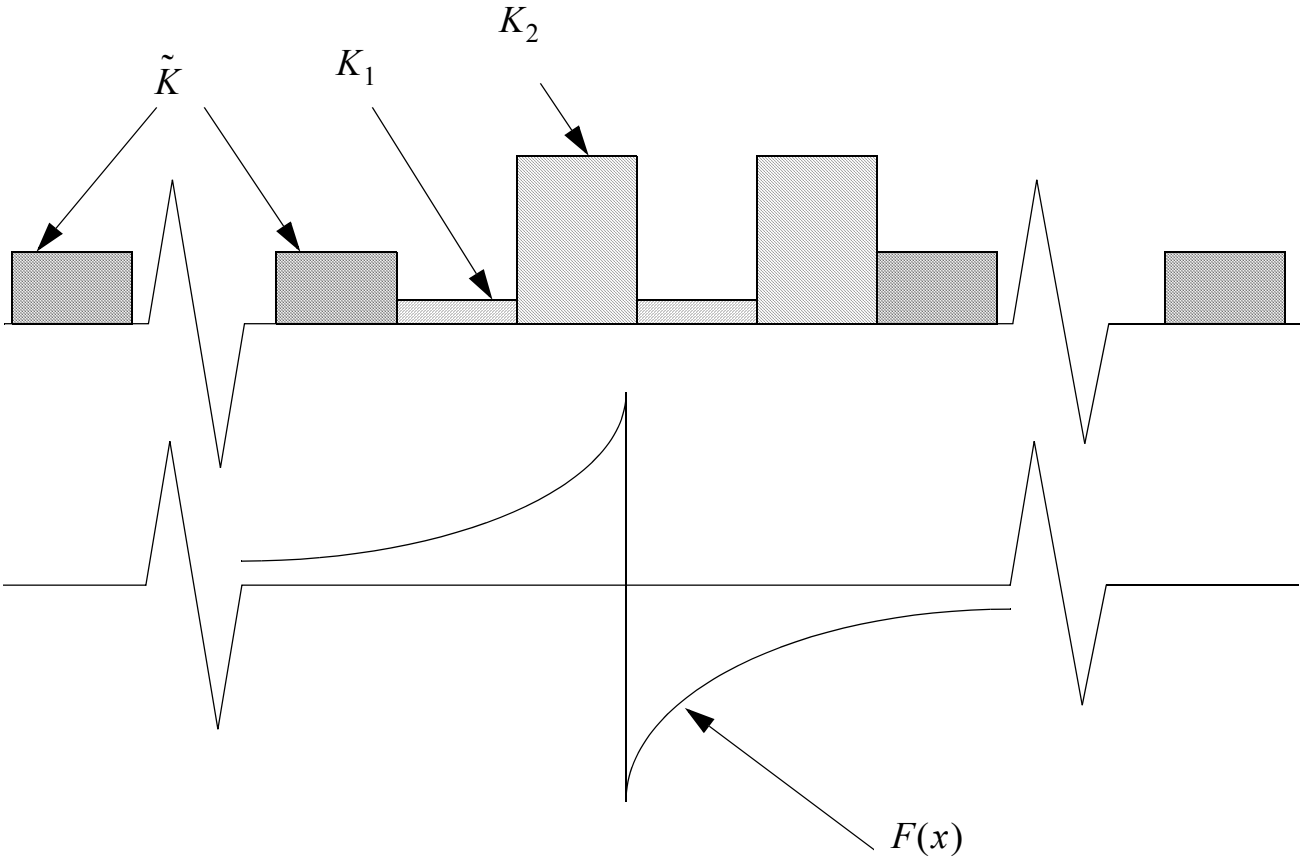

Table 1

q\k		1	2	3	4	5
0.1	k	0.0479	0.1743	0.3328	0.4630	10.0000
	$\tilde{n}-k$	19.9521	19.8257	19.6672	19.5370	
0.2	k	0.0480	0.1758	0.3387	0.4748	5.0000
	$\tilde{n}-k$	9.9520	9.8242	9.6613	9.5252	
0.3	k	0.0481	0.1775	0.3451	0.4880	3.3333
	$\tilde{n}-k$	6.6186	6.4892	6.3215	6.1787	
0.4	k	0.0482	0.1792	0.3520	0.5028	2.5000
	$\tilde{n}-k$	4.9518	4.8208	4.6480	4.4972	
0.5	k	0.0483	0.1809	0.3596	0.5198	2.0000
	$\tilde{n}-k$	3.9517	3.8191	3.6404	3.4802	
0.6	k	0.0484	0.1828	0.3678	0.5396	1.6667
	$\tilde{n}-k$	3.2849	3.1506	2.9655	2.7937	
0.7	k	0.0486	0.1847	0.3770	0.5633	1.4286
	$\tilde{n}-k$	2.8086	2.6725	2.4801	2.2938	
0.8	k	0.0487	0.1867	0.3872	0.5928	1.2500
	$\tilde{n}-k$	2.4513	2.3133	2.1128	1.9072	
0.9	k	0.0488	0.1888	0.3988	0.6320	1.1111
	$\tilde{n}-k$	2.1734	2.0334	1.8234	1.5902	
1.0	k	0.0489	0.1910	0.4122	0.6910	1.0000
	$\tilde{n}-k$	1.9511	1.8090	1.5878	1.3090	

Table 2

K_1/K_2	q	ρ^*	ρ_{100}	ρ_{100}^{conv}	ρ_{1000}	ρ_{1000}^{conv}
1/100	0.0392118	0.0099	0.0098	0.92278	0.00982	0.92253
1/1000	0.003992	0.000999	0.000992	0.99192	0.001001	0.99191

Table 3

K_1/K_2	q	num-berof unit cells	number of smoothing iterations	number of two-grid cycles
1/100	0.03921	100	2	20
			3	13
		1000	2	20
			3	13
1/10	0.3306	100	2	26
			3	20
		1000	2	26
			3	20
1/1	1.0	100	2	69
			3	46
		1000	2	69
			3	46

Table 4

num-ber of unit cells	number of smoothing iterations	number of two-grid cycles
100	2	16
	3	11
1000	2	16
	3	11

Table 5

K_1/K_2	N_e	N_c	N_0	ν_1, ν_2	ν_1^0, ν_2^0	type of the cycle	number of cycles
1/100	1,000	100	50	1	1	V	20
						W	20
				2	2	V	11
						W	11
				2	1	V	12
						W	11
				1	2	V	20
						W	20
1/100	10,000	1,000	500	1	1	V	20
						W	18
				2	2	V	10
						W	10
				2	1	V	10
						W	10
				1	2	V	18
						W	18
1/10	10,000	1,000	500	1	1	V	27
						W	27
				2	2	V	14
						W	14
				2	1	V	14
						W	14
				1	2	V	27
						W	27